AD-A145 124 ASSESSMENT OF THE STRESS CORROSION CRACKING OF POST-TENSIONED TENDONS AT T..(U) CONSTRUCTION ENGINEERING RESEARCH LAB (ARMY) CHAMPAIGN IL

UNCLASSIFIED E G SEGAN ET AL. JUN 84 CERL-TR-M-349 F/G 13/2 NL

1/1

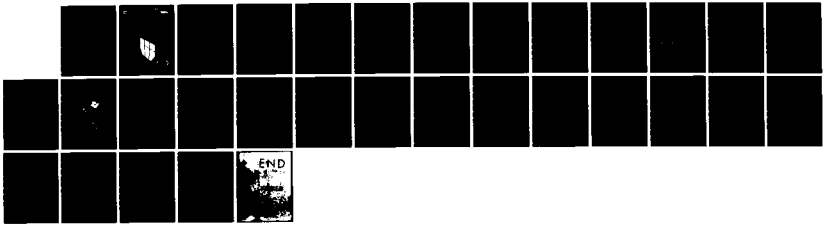

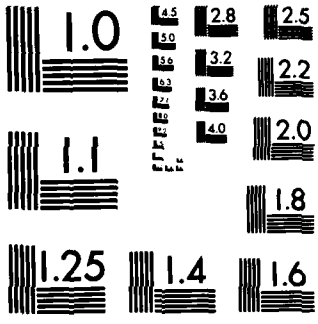

MICROCOPY RESOLUTION TEST CHART
NATIONAL BUREAU OF STANDARDS-1963-A

(12)

US Army Corps
of Engineers
Construction Engineering
Research Laboratory

AD-A145 124

Technical Report M-349
June 1984

ASSESSMENT OF THE STRESS CORROSION CRACKING OF POST-TENSIONED TENDONS AT THE JOHN DAY LOCK

by
E. G. Segan
D. Socie
D. Morrow

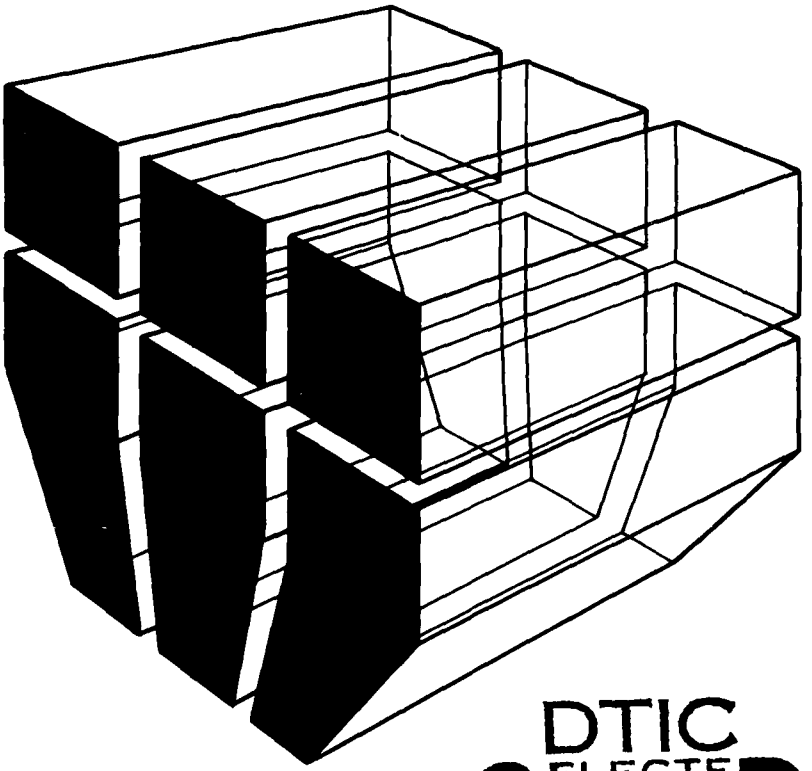

UNCLASSIFIED

SECURITY CLASSIFICATION OF THIS PAGE (When Data Entered)

REPORT DOCUMENTATION PAGE		READ INSTRUCTIONS BEFORE COMPLETING FORM
1. REPORT NUMBER CERL-TR-M-349	2. GOVT ACCESSION NO.	3. RECIPIENT'S CATALOG NUMBER
4. TITLE (and Subtitle) Assessment of the Stress Corrosion Cracking of Post-Tensioned Tendons at the John Day Lock		5. TYPE OF REPORT & PERIOD COVERED FINAL 6. PERFORMING ORG. REPORT NUMBER
7. AUTHOR(s) E. G. Segan D. Socie D. Morrow		8. CONTRACT OR GRANT NUMBER(s) IAO No. EN-DB-82-7 IAO No. E86830026 IAO No. E86830026 Ch. 1
9. PERFORMING ORGANIZATION NAME AND ADDRESS U.S. Army Construction Engr Research Laboratory P.O. Box 4005 Champaign, IL 61820-1305		10. PROGRAM ELEMENT, PROJECT, TASK AREA & WORK UNIT NUMBERS
11. CONTROLLING OFFICE NAME AND ADDRESS		12. REPORT DATE June 1984 13. NUMBER OF PAGES 26
14. MONITORING AGENCY NAME & ADDRESS(if different from Controlling Office)		15. SECURITY CLASS. (of this report) Unclassified 15a. DECLASSIFICATION/DOWNGRADING SCHEDULE

16. DISTRIBUTION STATEMENT (of this Report)

Approved for public release; distribution unlimited.

17. DISTRIBUTION STATEMENT (of the abstract entered in Block 20, if different from Report)

18. SUPPLEMENTARY NOTES

Copies are available from the National Technical Information Service
Springfield, VA 22161

19. KEY WORDS (Continue on reverse side if necessary and identify by block number)

John Day Lock
Locks (waterways)
stress corrosion

20. ABSTRACT (Continue on reverse side if necessary and identify by block number)

This report discusses research to determine the susceptibility of post-tensioned tendons to corrosion on repairs at the John Day Lock. The investigation assessed whether the repair system might fail due to stress corrosion cracking, investigated the rate at which this failure might occur, and recommended ways to reduce risk of system failure.

A high-strength wire used for post-tension cable meeting ASTM-A-416-74 specifications was found to be susceptible to general corrosion in aqueous environments and to

DD FORM 1 JAN 73 1473 EDITION OF 1 NOV 65 IS OBSOLETE

Unclassified

SECURITY CLASSIFICATION OF THIS PAGE (When Data Entered)

BLOCK 20. (Cont'd)

stress corrosion cracking in low-pH environments. The critical stress intensity factor for environmentally assisted attack, K_{ISCC}, was estimated to be about 15 to 30 ksi $\sqrt{in.}$ Critical flaw size to exceed K_{ISCC} was estimated at 0.010 in. Once steady-state crack growth at K greater than K_{ISCC} occurs, a single wire will fail in 16 to 166 hours. Since the remedial repair system has been in service for more than 2 years, it appears that steady-state crack growth stress corrosion cracking is not occurring and that the corrosion protection techniques already used have been effective.

A method of monitoring the remedial repair system for evidence of stress corrosion cracking was proposed in which tendons showing signs of water intrusion would be equipped with a load transducer for monitoring purposes. For long-term maintenance the number of shims added to each tendon would be recorded and the tendon replaced when they become excessive. Tendons would also be replaced if cumulative loss in pre-load becomes significant.

FOREWORD

This study was conducted for the Portland District of the U.S. Army Corps of Engineers under Intra-Army Order (IAO) No. EN-DB-82-7 dated 26 May 1982, IAO No. E86830026 dated 8 October 1982, and IAO No. E86830026, Change 1 dated 5 May 1983. The research was conducted by the Engineering and Materials (EM) Division, U.S. Army Construction Engineering Research Laboratory (CERL). Mr. Don Smith was the Portland District Technical Monitor. Dr. R. Quattrone is Chief of EM.

COL Paul J. Theuer is Commander and Director of CERL, and Dr. L. R. Shaffer is Technical Director.

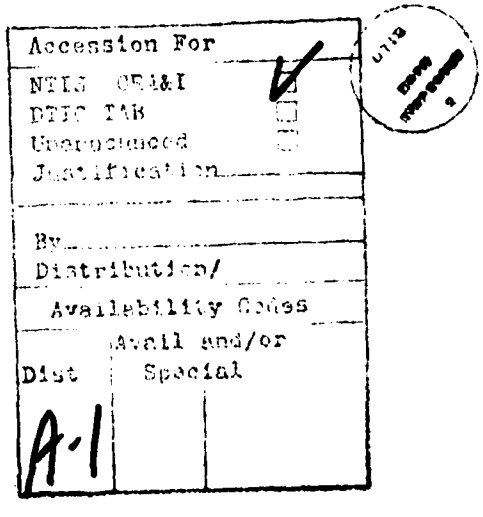

CONTENTS

TABLES

FIGURES

ASSESSMENT OF THE STRESS CORROSION CRACKING OF POST-TENSIONED TENDONS AT THE JOHN DAY LOCK

1 INTRODUCTION

Background

During the summer of 1981, the Portland District of the U.S. Army Corps of Engineers began remedial repair of the south lock wall of the John Day Lock and Dam, located in Oregon and Washington. The repair was needed to prevent excessive wall movement caused by the opening and growth of cracks at the wall base. The repair involved installing 45 post-tensioned tendons, stressed to 70 percent of their ultimate tensile strength, in the south wall of the lock nearly perpendicular to the cracks near the base.

The remedial repair was successful in reducing the lock wall movement. However, each time the lock is watered, water is forced through the tops of several assemblies and intrudes into some tendon assemblies. Migration of water up the tendon assemblies can expose the tendons to several types of corrosion. The greatest concern is that stress corrosion cracking (SCC) of the highly stressed wires could cause the remedial repair system to fail.

Objective

The objectives of this research were to (1) determine the susceptibility of the post-tensioned tendons to electrochemical corrosion and to SCC in aggressive environments resembling those to which the tendons are currently thought to be exposed, (2) assess whether the repair system might fail due to SCC, (3) assess the rate at which a failure could be expected to progress, and (4) recommend ways to reduce the risk of system failure.

Approach

The objectives of this research were met through a four-part program:

1. A standard metallurgical analysis was performed on tendon wire material taken from the lot used at the John Day Lock. Potentiodynamic scans were performed on the tendon wires and on a standard material (AISI 4130 steel, which is known to suffer from serious corrosion even in air); the relative corrosion resistance of the tendon material was assessed by comparing the results of the two sets of tests.

2. An investigation was made to determine the susceptibility of the tendon wire material used at the John Day Lock and Dam to SCC in solutions of the composition that could be expected in a pit or crevice. This was done by determining the time to failure of individual wires in the aggressive solutions as a function of initial stress and stress intensity. A material that is susceptible to SCC can be expected to fail under stress in an aggressive environment, even if the applied stress is well below the material's ultimate tensile strength. The goal of this part of the research was to determine the limits of stress on the wires that can lead to failure by SCC in aggressive environments.

3. The effect of stress corrosion cracking on the overall remedial repair system was evaluated, and the rate at which the failure of a tendon could be expected to progress was estimated.

4. A method for monitoring the remedial repair system was proposed, and appropriate actions to avoid future system failure were recommended.

2 COMPOSITION AND CORROSION SUSCEPTIBILITY OF TENDONS

Procedure

Samples of seven-strand tendon wire of the lot used for the John Day Lock and Dam were obtained from North Pacific Division, U.S. Army Corps of Engineers. Samples of the wire were chemically analyzed for major and minor constituents.

Potentiodynamic scans of the tendon wires and AISI 4130 steel were done to assess the relative corrosion resistance of the tendon materials to general corrosion. The potentiodynamic tests were conducted using a Princeton Applied Research (PAR) Model 350 corrosion measurement system. The tests were conducted in several types of solutions through which nitrogen was bubbled. The tests were done using a PAR Model 173 potentiostat/galvanostat with a Model 376 logarithmic current converter module and a standard Greene Cell. The samples of AISI 4130 steel were flat specimens having a 1 cm^2 of surface area; samples of the material were obtained from the tendon sample. Each sample was drilled and tapped to accept the Greene Cell sample holder and sealed against a teflon

sample holder. The samples were polished to a mirror finish before testing. The surface area of the tendon material specimens was determined by measuring the sample dimensions after polishing. Corrosion cell potentials were allowed to stabilize before starting the scans; the scans were done at a rate of 0.1 mV/s and terminated at potentials where the samples were visibly corroding rapidly. A saturated calumel electrode (SCE) was used as a reference for all electromotive force (emf) measurements.

Results and Discussion

Table 1 shows the results of the chemical analysis of the tendon materials. The analysis showed that the tendon material is a typical high-strength steel and that it contains no impurities outside the limits that would be expected for such a steel.

Table 2 summarizes the potentiodynamic scans performed on the tendon material and the standard material (AISI 4130 steel). Although the potentiodynamic scans do not directly measure the corrosion rate of a material, the scans may be used to assess the relative corrosion resistance of a material compared to that of another. AISI 4130 is a commonly used steel and, in many environments, suffers from general corrosion. The results of the potentiodynamic scans showed that the tendon steel behaves similarly to AISI 4130; the steel is highly sensitive to general corrosion, even in air. Thus, once it is exposed to a corrosive environment, corrosion can be expected to progress rapidly in the absence of inhibitors.

Table 1
Chemical Analysis of Tendon Wire

Element	Percent by Weight
Carbon	0.87
Manganese	0.66
Phosphorus	0.021
Sulfur	0.014
Silicon	0.29
Nickel	0.05
Chromium	0.12
Molybdenum	0.01
Copper	0.03
Spectrographic Tramp Element Survey (amounts indicated are approximate)	
Aluminum	0.005
Titanium	T* < 0.005
Vanadium	0.005
Tin	0.007
Cobalt	T* < 0.005

*T Trace.

Table 2
Summary of Corrosion Resistance Tests

Material	*Environment*
Tendon wire	pH = 3 HCl
Tendon wire	3.5 percent NaCl
Tendon wire	Doctored Water
AISI 4130 steel	pH = 3 HCl
AISI 4130 steel	3.5 percent NaCl
AISI 4130 steel	Doctored Water

3 SUSCEPTIBILITY OF TENDONS TO STRESS CORROSION CRACKING

The requirements for stress corrosion cracking (SCC) involve only three criteria: the presence of a high enough stress, a material that is susceptible to SCC, and an environment that is favorable for SCC.

Figure 1 shows the typical configuration of a tendon in the lock wall. The tendons are made of high-strength steel that is susceptible to SCC in many environments. The tendons were not intended to be exposed to an aqueous environment; migration of water up the tendons is the result of failure of waterproofing at some location(s) in the assembly. The point of water intrusion appears to be at the top of the tendon anchorage. At this time, the condition of a tendon's wires can be assessed only by destructive testing (i.e., by pulling a tendon out of the wall). This method is only marginally useful; although SCC in that tendon may be identified, the condition of the other tendons is still unknown. Chemical analysis of water leaving the top of the tendon assemblies after watering of the lock shows that chloride levels are low, calcium levels are high, and the pH is 11 to 12—well within the "safe" range for avoiding SCC of steel in concrete or grout environments. The remedial repairs have operated for 2 years without incident, and the intended goal of the repair system has been achieved (i.e., lock wall movement during watering and dewatering has been minimized).

The probability of grease flowing or severe grout cracking increases over time, so the likelihood of

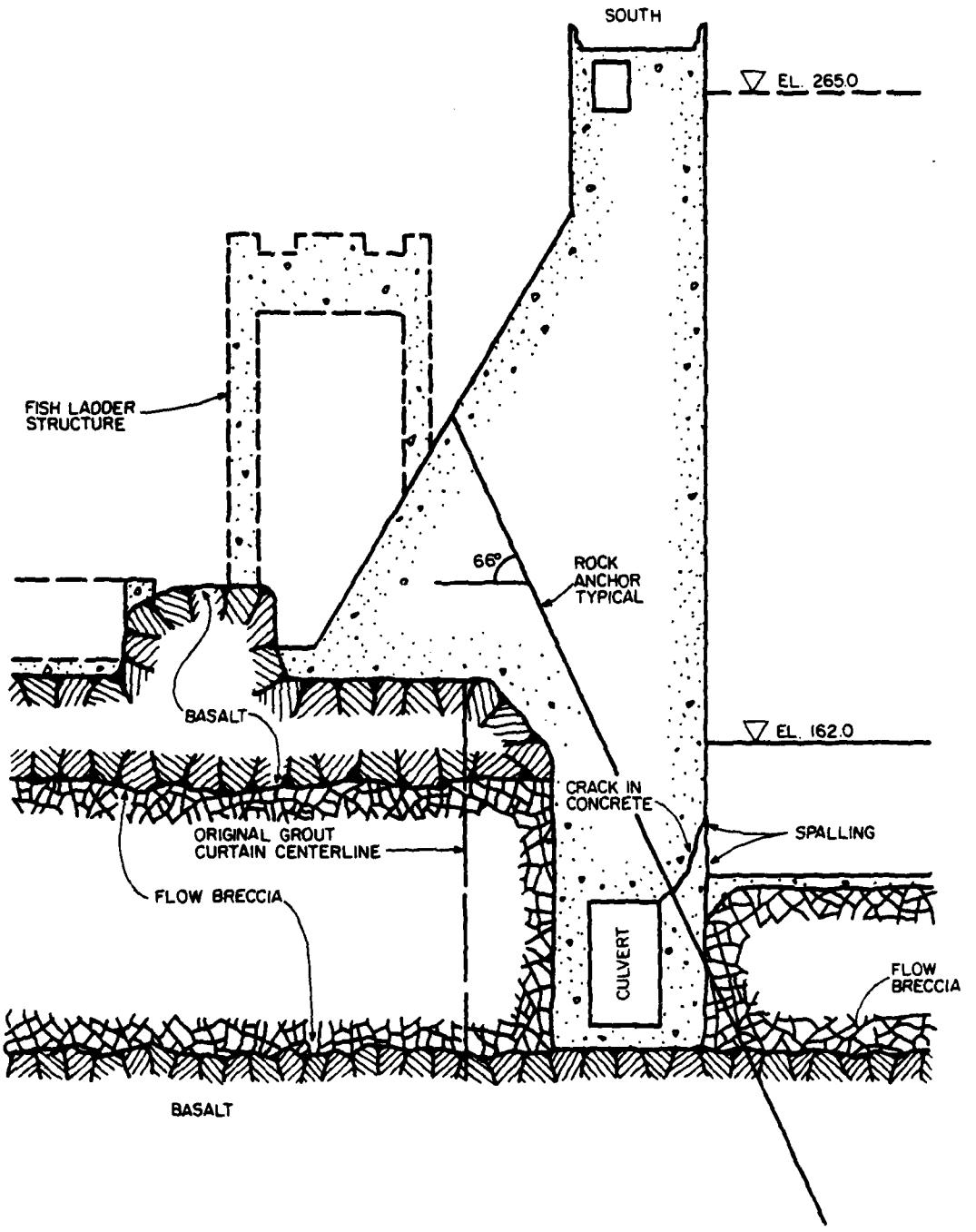

Figure 1. Schematic diagram of John Day Lock and Dam showing cracks in south wall of lock and placement of post-tensioned tendons.

direct contact of the water with the steel increases. The pH of water in the assemblies may be much lower than that measured at the top assemblies. When the lock is dewatered, hydrostatic pressure forces the water out of the assemblies and, as the water recedes, it mixes with air. This can decrease the pH of the solution. The pH in a pit or crevice is about 3 to 4 and is relatively independent of the bulk of the solution through a wide pH range (often up to pH = 10 to 12).[1] Pits or crevices that were present in the steel when installed or which formed since installation can contain very aggressive environments; once pits are formed, SCC occurs when the surface defects gradually sharpen under the applied stress to form a crack. Once the cracks are initiated (a process that can take years), they can grow under the applied stress until they reach the critical size for wire failure.

Stress Corrosion Cracking of Individual Wires

To estimate the critical crack size and the threshold stress intensity for environmentally assisted crack growth (K_{ISCC}), individual wires were notched and tested in pH 3 HCl. Samples for SCC studies were mounted in Cortest proof rings. These fixtures provide a constant stress on the specimen that is linearly proportional to the deflection of the ring for small specimen strains. Specimens were loaded to the desired stresses and corrosive media were placed in the environmental chamber. Samples for this investigation were about 2 in.* long; they were machined to a diameter of 0.130 in. for about 3/4 in. gage length in the center to insure fracture within the corrosive medium.

The initiation time for the formation of sharp cracks in pH 3 HCl and in 3.5 percent NaCl solution was too long to yield sufficient data during the time span of this investigation. Even samples that were notched by cutting with a diamond saw failed to yield critical-size cracks after 4 to 5 weeks of immersion in the test solutions at high stresses (>0.8 of the ultimate tensile strength). However, this behavior does not necessarily imply that the steel is immune to SCC; the initiation time may take months or even years.

The research program was modified to yield statistically representative data in a shorter period of time. Samples were notched by cutting with a diamond saw, and sharp cracks were initiated by fatigue. The size of a crack in a material greatly affects its ability to bear load. Conventionally, fracture mechanics uses the stress intensity factor to quantify a material's strength while allowing for the presence of cracks of various sizes and shapes. The stress intensity factor, K, has the form:

$$K = P\sqrt{a}f(a) \qquad \text{[Eq 1]}$$

where:

P = applied load
a = crack length
f(a) = geometry constant for given crack length.

The critical stress intensity factor (K_{IC}), a material property, describes the stress intensity at the tip of a sharp crack that will produce failure in a noncorrosive medium. Since K_{IC} at fracture is constant, Eq 1 shows that for an applied load below the ultimate tensile strength, a material can fracture if the crack size becomes large enough. This analysis holds only for a specific set of geometries and for "automatically" sharp cracks. For example, fatigue cracks are considered to be automatically sharp; a cut by a saw does not result in a sharp crack.

The strength of a material in a corrosive environment is defined by the critical stress intensity factor for SCC (K_{ISCC}). If a material is not susceptible to SCC, its K_{ISCC} will be equal to K_{IC}; if it is susceptible, its K_{ISCC} can be much lower than K_{IC}.

Stress Corrosion Cracking of Wires at the John Day Lock

The Appendix contains specific information on the John Day Lock. It includes a section on the derivation of equations used for sample geometry, a printout of a program to calculate K for varying sample radii and applied loads, and a tabulation of K as a function of applied load for samples with radii of 0.065 in. and 0.1 in.

Pre-cracked samples were loaded to various stress levels in the test rings and submerged in pH 3 HCl. Ten samples failed as they were being loaded. These samples represent the value of K at a time to rupture of zero (i.e., $K_{ISCC} = K_{IC}$ at t = 0). The time to failure for these tests was recorded electronically. Table 3 shows the time to failure and estimated initial stress intensity for this test. An initial crack size of 0.050 in. was assumed for all but the zero-time-to-failure specimens. Figure 2 shows a plot of the estimated stress intensity as a function of time to failure. From the

[1] B. F. Brown, ed., *Stress Corrosion Cracking in High Strength Steels and in Titanium and Aluminum Alloys* (Naval Research Laboratory, 1972), pp 2-16.

*1 in. = 25.4 mm.

Table 3
Time to Failure Data

Time (hr)	K (ksi $\sqrt{in.}$)	Time (hr)	K (ksi $\sqrt{in.}$)
0	157.9	95	66.7
0	207.5	96	73.7
0	75.0	26	51
0	77.1	21	107
0	207.5	113	62.2
0	104.8	436	96
0	111.7	44	51
0	80.9	415	62
0	88.1	352	51
0	113.7	362	90.8
2712	67.8	47	73.7
77	56.7	1284	67.7
839	45	24	62
3456	56.7	144	84.8
48	39.6		
51.7	45		
499.3	79		
24	113		
19	56.7		

plot, the value of K_{Ic} can be estimated at 120 ksi $\sqrt{in.}$ Some tests are still being run and are indicated by an X with an arrow pointing toward the right. At very long times (greater than 1000 hr), the value of stress intensity below which failure does not occur can be estimated to be between 15 and 30 ksi $\sqrt{in.}$ This is a typical value for high-strength steels with a yield of about 200 ksi. For example, K_{ISCC} for D6AC steel with a 220-ksi yield is estimated to be 36 ksi $\sqrt{in.}$ in 3 percent NaCl.[2]

This phase of the research has shown that the high-strength steel meeting ASTM-A-416-74 specifications is susceptible to SCC and that K_{ISCC} is about 15 to 30 ksi $\sqrt{in.}$

4 THE EFFECT OF STRESS CORROSION CRACKING ON THE REMEDIAL REPAIR SYSTEM

The remedial repair system may fail in several ways. Failure may occur when the tendons cease to control the lock wall movement within the desired limits during watering and dewatering, when the seepage rate of water between the interior of the lock and the culvert reaches unacceptable levels, or from other causes. The definition of system failure can be subjective (i.e., depending on the judgment of the lock operators). However, each mode of failure may be characterized by the failure of a critical number and combination of individual tendons. Presumably, these calculations have already been made.

The critical flaw or crack size required to exceed K_{ISCC} can be estimated from the value determined for K_{ISCC}. If a value of 30 ksi $\sqrt{in.}$ is used for K_{ISCC} and a working load of 6 kip is used, the crack needed to exceed 30 ksi $\sqrt{in.}$ is about 0.010 in. Corrosion cracks or flaws that are greater than 0.010 in. would allow the wire to undergo steady crack growth in low pH environments, such as a corrosion pit.

The *Damage Tolerant Design Handbook*[3] provides an estimate of steady crack growth rate for several high-strength steels. The crack growth rates are all about 10^{-6} to 10^{-7} in. sec. This is a very rapid rate and is nearly independent of stress intensity for values above K_{ISCC}. For the 0.2-in.-diameter wires under a working load of 6 kips, failure will occur when the crack reaches about 0.070 in. (i.e., $K = K_{Ic}$ when $a = 0.070$). Thus, the amount of crack growth needed for failure is only 0.060 in. If the crack grows at 10^{-6}

[2] J. F. Campbell, W. E. Berry, and C. F. Feddersen, *Damage Tolerant Design Handbook* (Metals and Ceramics Information Center, Battelle Columbus Laboratories, 1972).

[3] J. F. Campbell, W. E. Berry, and C. F. Feddersen.

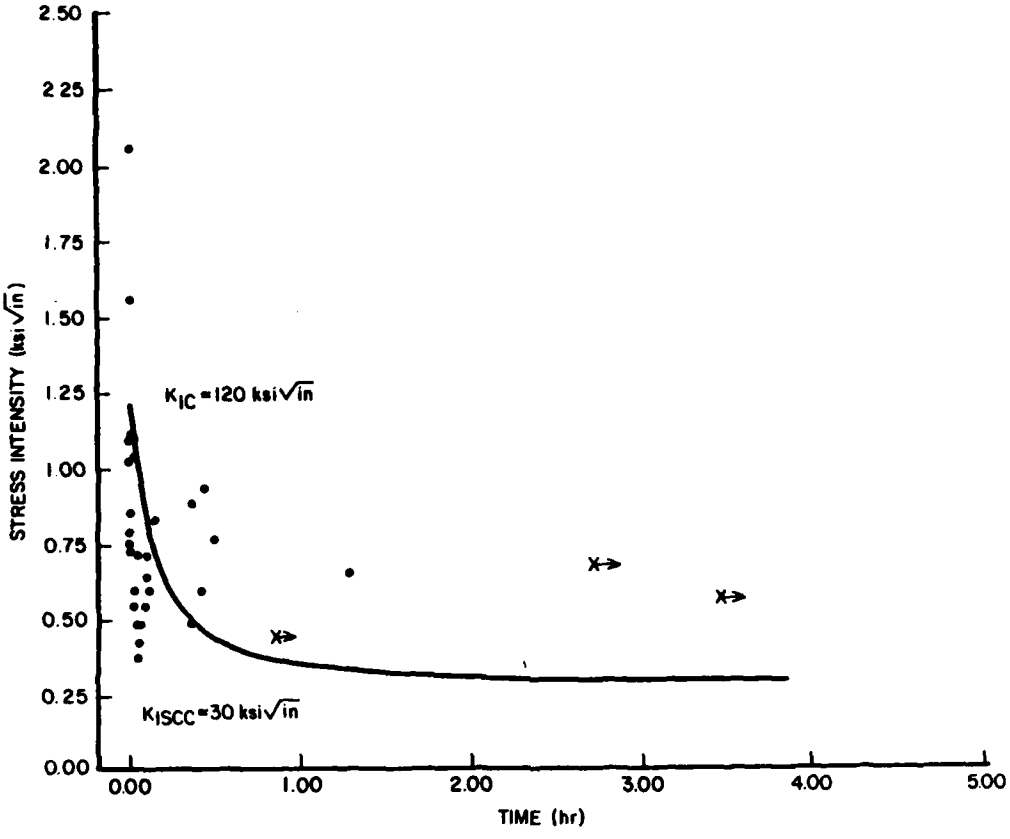

Figure 2. Observed stress intensity versus time to failure observed in laboratory for tendon material used at John Day Lock.

to 10^{-7} in./sec., the affected wire will fail in only 16 to 166 hours.

The remedial repair system implemented at the John Day Lock and Dam has been in service for more than 2 years with no failures from SCC. This suggests that there is no steady crack growth SCC in the repair system. The corrosion protection used (grease coating and grouting) appears to be effective. Griess and Naus[4] have investigated these coatings on ASTM-A-416-74 cable in aggressive environments and found them to offer complete protection from corrosion as long as the grease is not flowing out of the system or the grout badly cracked (i.e., cracks longer than 0.04 in.). The John Day Lock cables were greased and covered with a plastic sheath and then set in secondary grout above the primary grout packer (see Figure 3). Below the primary grout packer, the bare wires were anchored with a primary grout of Porland cement. Since the bare wires in the primary grout region are protected only by the primary grout, this area would present problems if the grout became badly cracked. On the other hand, the grout in this region must be in compression to keep the tendon in place, and cracks which do occur

[4] J. C. Griess and D. J. Naus, "Corrosion of Steel Tendons Used in Prestressed Concrete Pressure Vessels," in D. E. Tonini, American Hot Dip Galvanizers Assn., Inc., J. M. Gaidis, and W. R. Grace & Co., eds., *Corrosion of Reinforcing Steel in Concrete*, ASTM Special Technical Publications 713 (ASTM, 1980), pp 32-50.

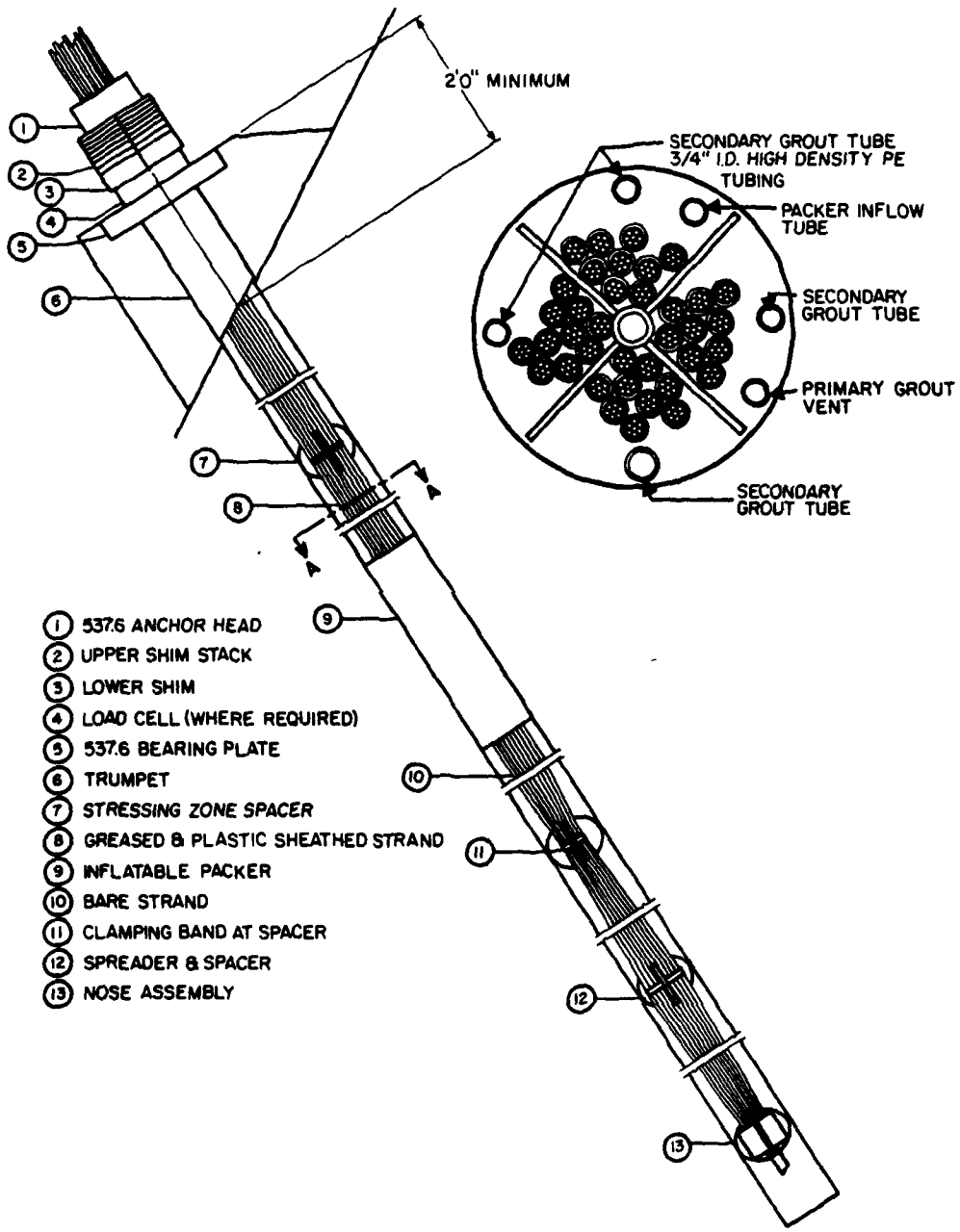

Figure 3. Schematic diagram of tendon used for remedial repair.

should be held closed; thus, the SCC problem should be eliminated in this case.

Another region of concern is the anchor head area. During normal watering and dewatering cycles, this area is exposed to alternating wet and dry conditions. Extra care must be taken to insure that all tendon components above the secondary grout are continuously coated with corrosion-inhibiting grease.

It is unlikely that all of the grease will flow or all the grout will crack severely in any one location. Thus, there is no reason to expect an entire tendon (37 cables) to fail at once.

Figure 4 shows the tendon response to both constant load (assuming the pre-load equals the fully watered load) and constant displacement (fully dewatered). For the fully watered or constant load case, the ratio of current stress to original pre-stress versus number of broken strands indicates an unstable response after 11 strands (77 wires) have failed. Since the stage II crack growth rate (Figure 5) is nearly independent of stress intensity, the stress shedding from

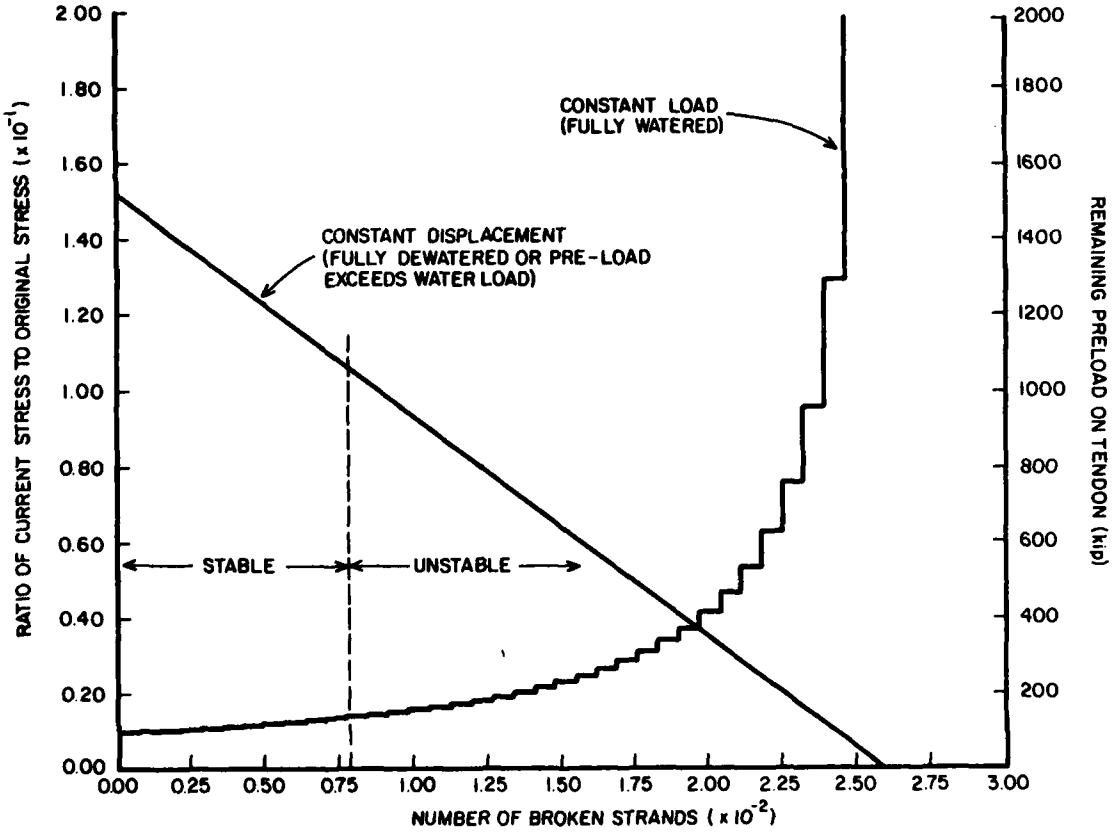

Figure 4. The effect of number of broken strands in tendon on ratio of current stress on tendon to original stress.

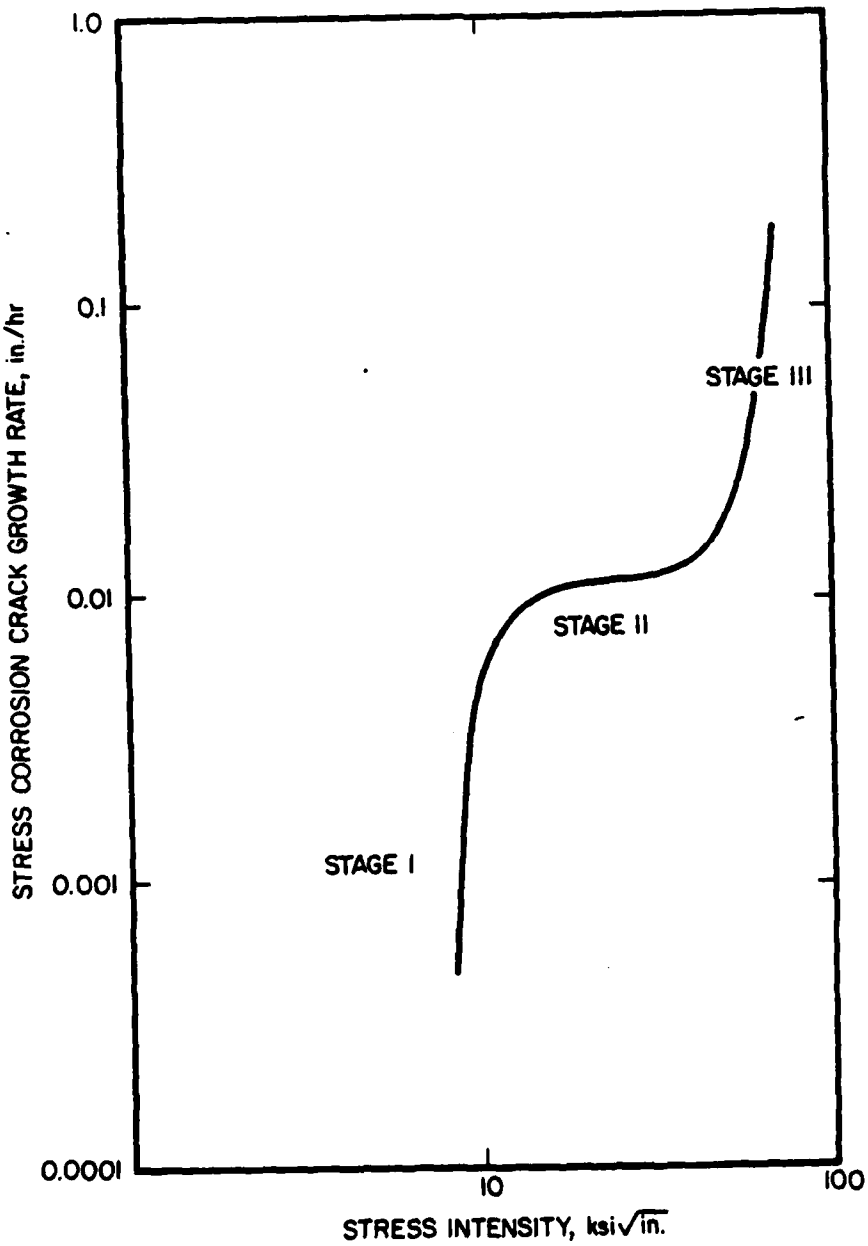

Figure 5. The effect of stress intensity at crack tip on crack growth rate.

failed wires will only accelerate the incubation period and not the crack growth rate. At least 77 wires would have to enter stage III crack growth while the lock is fully watered to cause catastrophic failure of a tendon. If each strand (7 wires) entered stage II crack growth sequentially, the estimated time from the first sign of failure to complete tendon failure would be about 160 to 1600 hours (i.e., 10 strands times the time to fail per wire). This estimate assumes that all wires in each strand will fail at exactly the same time. The estimated time range of 160 to 1600 hours should allow ample opportunity to dewater the lock and begin repairs. Figure 4 also shows the constant displacement response of a tendon which is representative of the lock in the dewatered state or while the pre-load exceeds the watering loads. This plot of remaining load vs. number of strands failed demonstrates that upon watering, the pre-load will drop almost 30 percent before the tendon will fail.

It should be noted that the stress on the tendons prevents tendon fatigue during watering and dewatering of the lock because the high stresses prevent the opening and closing of the cracks in the lock wall. The temptation to reduce the stress on the tendons to prevent SCC should be avoided, because this could lead to cyclic loading of the tendons. This would ultimately lead to corrosion fatigue, which is a more serious problem than SCC. All the analyses performed for the tendons have been based on the assumption of constant, not cyclic loading. If there is evidence of SCC during the periodic inspections, the tendons should be extracted from the structure and replaced; the load should never be reduced to minimize the stress while the remedial repair system is operating.

5 A METHOD TO MONITOR THE REMEDIAL REPAIR SYSTEM

All tendons showing signs of water intrusion should be equipped with a load transducer for monitoring purposes. Figure 4 suggests that the amount of load drop in the tendon would be a good indication of the tendon's condition. Significant drops in load due to loss of net section area would be about 40 kips (the load per strand) and should be easily detected. For long-term maintenance, a record should be kept of the number of shims added to each tendon to maintain pre-load. If the rate of shimming in in./yr. changes or the total current displacement with respect to the 10 percent datum measured during installation of the tendons becomes excessive, the tendon should be replaced. If 11 strands fail, the displacement is about three times the original displacement. Since this is an unstable condition, the shim displacement should never be allowed to approach this value. Also, any loss in pre-load between maintenance intervals should be recorded: if the cumulative loss in pre-load becomes significant, the tendon should be replaced.

6 CONCLUSIONS AND RECOMMENDATIONS

This research has produced the following conclusions:

1. The high-strength wire used for post tension cable meeting ASTM-A-416-74 specifications was found to be susceptible to general corrosion in aqueous environments and to stress corrosion cracking in low-pH environments. The critical stress intensity factor for environmentally assisted attack (K_{ISCC}) was estimated to be about 15 to 30 ksi $\sqrt{in.}$

2. The critical flaw size to exceed K_{ISCC} was estimated at 0.010 in. It was estimated that once steady-state crack growth is entered at K greater than K_{ISCC}, a single wire in a tendon will fail in 16 to 166 hours.

3. Since the remedial repair system has been in service more than 2 years, it appears that steady-state crack growth stress corrosion cracking is not occurring and that the corrosion protection techniques already used have been effective.

4. Corrosion fatigue of the tendons does not appear to be a factor as long as a high enough load is maintained on the tendons to prevent the opening of the cracks at the wall's base.

5. The analysis showed that SCC may occur on two regions of the tendons: (1) the primary grout region, and (2) the anchor head area, which is exposed to alternating wet and dry conditions as the lock is watered and dewatered.

On the basis of this research, the following recommendations are made:

1. Maintain the anchor head areas by insuring that the inhibiting grease coatings are maintained periodically.

2. Do not reduce the stress on the tendons while the remedial repair system is operating.

3. Monitor and maintain the tension in the tendons at regular intervals as long as the remedial repair system is used. This may be done by:

a. Noting the rate of shimming required to maintain the desired stress in in./yr. In this case, a change in compliance because of decrease in net section area would be evident by a change in the amount of shimming required to maintain the desired load.

b. Equipping all tendons showing signs of water intrusion with load transducers to help detect loss of pre-load. It was estimated that significant drops in load due to loss of net section area would be about 40 kips (the load per strand), which is easily detectable.

4. If SCC of a particular tendon is discovered during the periodic inspections, the tendon should be removed and replaced.

REFERENCES

Brown, B. F., ed., *Stress Corrosion Cracking in High Strength Steels and in Titanium and Aluminum Alloys* (Naval Research Laboratory, 1972), pp 2-16.

Campbell, J. E., W. E. Berry, and C. E. Feddersen, *Damage Tolerant Design Handbook* (Metals and Ceramics Information Center, Battelle Columbus Laboratories, 1972).

Griess, J. C. and D. J. Naus, "Corrosion of Steel Tendons Used in Prestressed Concrete Pressure Vessels," in D. E. Tonini, American Hot Dip Galvanizers Assn., Inc., J. M. Gaidis and W. R. Grace & Co., eds., *Corrosion of Reinforcing Steel in Concrete*, ASTM Special Technical Publications 713 (ASTM, 1980), pp 32-50.

APPENDIX: ESTIMATING MODE I STRESS INTENSITIES FOR EDGE NOTCHED ROUNDS TESTED BY CERL

The specimens tested by CERL to determine the susceptibility of the tendon wire to SCC were single edge notched rounds. The notch was cut by a diamond saw to the depth of 0.040 in. A sample midsection is shown in Figure A1. Without experimentally determined K-calibration data, the values of stress intensity for this geometry can only be estimated.

The approach taken in this work was to model the edge notched round as an edge notched plate of which there is a known solution for K_I. Figure A2 depicts a cracked specimen. Two important characteristics were preserved when going from the round to the rectangular cross-sections. First, the crack front was used as the thickness dimension for the plate solution and, second, the depth of the plate was selected so the edge cracked plate had the same crack length and bending stiffness as the edge notched round. Once the equivalent bending stiffness was determined, the values of h, b, and a were determined for the solution shown (from ASTM-STP 410 [1969]) in Figure A3.

Next, the depth of a rectangular cross-section with width h and crack length a is computed such that the bending stiffness is the same as the round cracked specimen. The equivalent bending stiffness is determined with respect to the centroidal axis of the uncracked material as follows:

$$\frac{I_{round}}{y_{round}} = \frac{I_{rectangular}}{y_{rectangular}}.$$

Using Figure A3 as a guide, consider a plate of finite width b and thickness h containing a single-edge crack of length a perpendicular to the edge. The plate is subjected to a tensile force P. The stress intensity factor can be written as

$$\text{For} \left(\frac{a}{b}\right) \leq 0.6$$

$$k_1 = \frac{P\sqrt{a}}{bh\sqrt{\pi}} \left[1.99 - 0.41\left(\frac{a}{b}\right) + 18.70\left(\frac{a}{b}\right)^2 - 38.48\left(\frac{a}{b}\right)^3 + 53.85\left(\frac{a}{b}\right)^4\right]$$

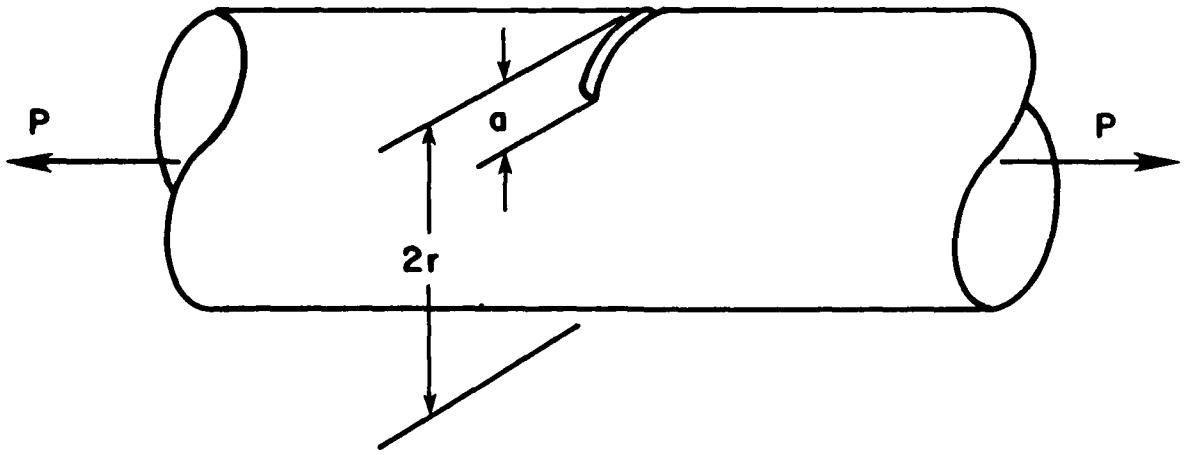

Figure A1. Single edge notched round for testing.

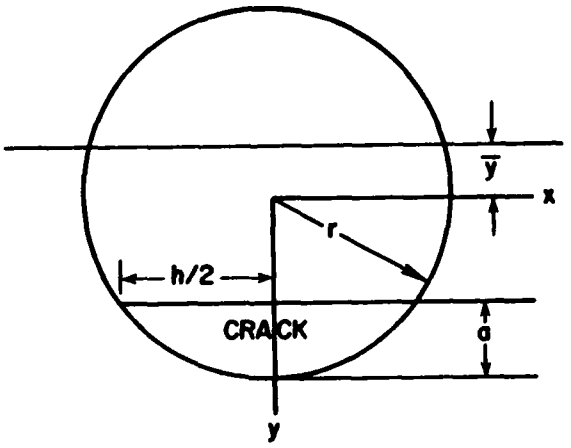

Figure A2. Cracked specimen, in which h is the thickness of the plate and is determined as $h = 2(r^2 - (r-a)^2)^{1/2}$.

Figure A4 shows an equivalent rectangular cross-section. For this section

$$\bar{I}_r = \frac{h(b-a)^3}{12}$$

and

$$y_r = \frac{b-a}{2}.$$

Thus

$$\frac{\bar{I}_r}{y_r} = \frac{h(b-a)^2}{6}.$$

The bending stiffness of the round specimen is

$$\frac{\bar{I}_{md}}{y_{md}}$$

where y_{md} is either $r - a + \bar{y} \rightarrow$ compressive or $r - y \rightarrow$ tensile. Equating the two bending stiffness relations yields

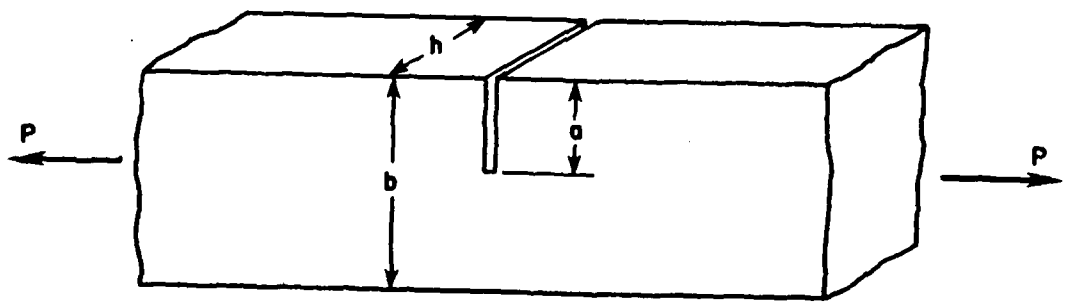

Figure A3. Single edge cracked plate under tension. (From ASTM-STP 410 [1969].)

$$\frac{\bar{I}_{rnd}}{r - \bar{y}_{rnd}} = \frac{h(b-a)^2}{6}$$

or

$$b = \left[\frac{I_{rnd}\,6}{(r - y_{rnd})h}\right]^{1/2} + a.$$

Next the values of $\bar{I}_{rnd}$ and $\bar{y}_{rnd}$ must be determined as follows:

$\bar{y} = \dfrac{\int y\,dy\,dx}{A}$ definition of centroid of an area;

$I_x = \int y^2 dA$ definition of moment of inertia with respect to x-axis;

$\bar{I} = I_x - A\bar{y}^2$ parallel axis theorem to find $\bar{I}$ where A is the remaining area of the round specimen.

$$A = \pi r^2 - A_{crack}$$

where

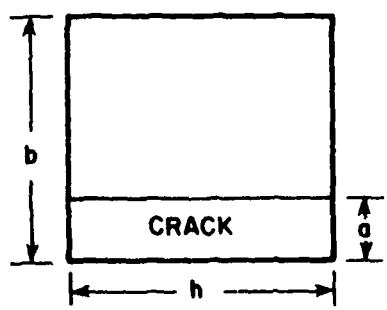

Figure A4. Cross-section of cracked rectangular specimen.

$$A_{crack} = 2 \int_{r-a}^{r} \int_{0}^{(r^2 - y^2)^{1/2}} dydx$$

$$A_{crack} = 2\left[\frac{r^2\pi}{4} - \frac{(r-a)[r^2 - (r-a)^2]^{1/2}}{2} - \frac{r^2}{2}\sin^{-1}\left(\frac{r-a}{r}\right)\right]$$

$$y = \frac{\int ydydx}{A} = \frac{\frac{2}{3}(r^2 - (r-a)^2)^{3/2}}{A}$$

Then

$$I_x = \int y^2 dA = \int_{-(r-a)}^{r} \int_{-(r^2-y^2)^{1/2}}^{(r^2-y^2)^{1/2}} y^2 dxdy$$

$$I_x = 2\left\{\frac{r^4\pi}{16} - \left[\frac{(a-r)}{8}(2(a-r)^2 - r^2)(r^2 - (a-r)^2)^{1/2} + \frac{r^4}{8}\sin^{-1}\left(\frac{a-r}{r}\right)\right]\right\}$$

From this the value of $\bar{I}$ can be computed:

$$\bar{I} = I_x - A\bar{y}^2.$$

This solution was run on a computer for a range of crack lengths from 0 to 0.098 in. The program written in BASIC and the values for h, b and K as a function of crack length are shown in Figures A5, A6, and A7.

Two solutions were run. Figure A6 depicts a 0.065 in. radius which corresponds to the specimen geometry. Figure A7 shows a 0.1 in. radius which corresponds to the actual wire geometry. These reference tables were used in this report to estimate stress intensity for given crack sizes.

```
 10 ! CERL DATA REDUCTION
 20 ! 10/31/83 D.L.M
 30 OPTION BASE 1
 40 DIM C(100),Q(100),A(100),X(1
    00)
 45 DIM Y(100),X1(100)
 50 N=99 !
 70 DISP "ENTER RADIUS OF SAMPLE
    S" @ INPUT R
 71 C=0
 80 FOR I=1 TO N
 90 ! DISP "CRACK LENGTH(in) OF
    SAMPLE#";I
100 ! INPUT C(I)
101 C(I)=C
102 C=C+.001
110 NEXT I
198 !
199 !
200 ! COMPUTE Qx
210 FOR I=1 TO N
220 Q(I)=2/3
230 Q(I)=Q(I)*(R^2-(R-C(I))^2)^(
    3/2)
240 NEXT I
298 !
299 !
300 ! COMPUTE AREA REMAINING
310 FOR I=1 TO N
320 A1=R*R*PI/4
330 A2=(R-C(I))/2
340 A3=(R*R-(R-C(I))^2)^.5
350 A3=A3/2
360 A4=R*R*ASN((R-C(I))/R)
370 A4=A4/2
380 A(I)=PI*R*R-2*(A1-A2*A3-A4)
390 NEXT I
398 !
399 !
400 ! COMPUTE Ix
410 FOR I=1 TO N
420 I1=R^4*PI/16
430 I2=C(I)-R
440 I2=I2/8
450 I3=2*(C(I)-P)^2-R^2)
460 I4=(P^2-(C(I)-R)^2)^.5
470 I5=R^4*ASN((C(I)-R)/R)
480 I5=I5/8
490 X(I)=2*(I1-I2*I3*I4-I5)
497 NEXT I
498 !
499 !
500 ! COMPUTE CENTROID
510 FOR I=1 TO N
520 Y(I)=Q(I)/A(I)
530 NEXT I
598 !
599 !
600 ! USE AXES SHIFT FORMULA
610 FOR I=1 TO N
620 X1(I)=X(I)-A(I)*Y(I)^2
630 NEXT I
698 !
699 !
700 ! OUTPUT DATA
710 GOSUB 765
735 IMAGE Z.3D,X,D.3DE,X,D.3DE
740 FOR I=1 TO N
750 PRINT USING 735 ; C(I),Y(I),
    X1(I)
755 IF I=50 THEN GOSUB 765
760 NEXT I
761 GOTO 799
765 PRINT @ PRINT @ PRINT @ PRIN
    T
766 PRINT "CRACK Y-BAR          I-BA
    R"
767 PRINT "  in    (in^4)      in
    ^4)"
769 PRINT "------ ---------- ----
    ------"
770 RETURN
798 !
799 !
800 ! OUTPUT DATA
810 GOSUB 865
835 IMAGE D.3DE,X,ZZ.3D,2X,Z.3D
840 FOR I=1 TO N
841 IF Y(I)=0 THEN PRINT @ GOTO
    860
842 X=(R*R-(R-C(I))^2)^.5
843 B=C(I)+(3*X1(I)/(X*(R-Y(I)))
    )^.5
844 H=2*X
849 IF Y(I)=0 THEN 860
850 PRINT USING 835 ; X1(I)/Y(I)
    ,B,H
855 IF I=50 THEN GOSUB 865
860 NEXT I
861 GOTO 899
865 PRINT @ PRINT @ PRINT @ PRIN
    T
867 PRINT "I/y          b       h
    "
869 PRINT "Fraction  (width) th
    ick)"
870 PRINT "---------- ----------
    ----"
871 RETURN
898 !
899 !
900 ! OUTPUT DATA K(mode 1)
910 GOSUB 965
935 IMAGE "(",Z.3DE,")P"
940 FOR I=1 TO N
941 IF Y(I)=0 THEN PRINT @ GOTO
    960
942 X=(R*R-(R-C(I))^2)^.5 @ H=2*
    X
943 B=C(I)+(3*X1(I)/(X*(R-Y(I)))
    )^.5
945 K1=C(I)^.5/(B*H*PI^.5)
946 K2=K1*(1.99-.41*K+18.7*K^2-3
    8.48*K^3+53.85*K^4)
950 PRINT USING 935 ; K2
955 IF I=50 THEN GOSUB 965
960 NEXT I
961 GOTO 980
965 PRINT @ PRINT @ PRINT @ PRIN
    T
967 PRINT " Stress Intensity "
969 PRINT " (ksi[in.])^1/2)"
970 PRINT " ----------------
    "
971 RETURN
980 END
 22794
```

Figure A5. BASIC program and values for h, b, and K as a function of crack length.

Radius of Samples
0.065 in.

CRACK (in.)	Y-BAR (in^4)	I-BAR (in^4)	I/stiffness	b (width)	h (thick)	Stress Intensity (Ksi[in]^1/2)
0.000	0.000E+000	1.402E-005				
0.001	7.575E-005	1.319E-005	1.741E-001	00.233	0.023	(6.714E+000)P
0.002	2.146E-004	1.278E-005	5.956E-002	00.194	0.032	(8.065E+000)P
0.003	3.938E-004	1.243E-005	3.155E-002	00.175	0.039	(8.997E+000)P
0.004	6.050E-004	1.210E-005	1.999E-002	00.162	0.045	(9.739E+000)P
0.005	8.431E-004	1.178E-005	1.397E-002	00.153	0.050	(1.038E+001)P
0.006	1.105E-003	1.147E-005	1.039E-002	00.147	0.055	(1.095E+001)P
0.007	1.387E-003	1.117E-005	8.057E-003	00.141	0.059	(1.147E+001)P
0.008	1.688E-003	1.088E-005	6.447E-003	00.136	0.062	(1.197E+001)P
0.009	2.005E-003	1.059E-005	5.281E-003	00.133	0.066	(1.246E+001)P
0.010	2.338E-003	1.030E-005	4.406E-003	00.129	0.069	(1.293E+001)P
0.011	2.686E-003	1.002E-005	3.732E-003	00.126	0.072	(1.341E+001)P
0.012	3.046E-003	9.744E-006	3.199E-003	00.124	0.075	(1.388E+001)P
0.013	3.418E-003	9.471E-006	2.770E-003	00.122	0.078	(1.436E+001)P
0.014	3.802E-003	9.201E-006	2.420E-003	00.120	0.081	(1.484E+001)P
0.015	4.196E-003	8.935E-006	2.129E-003	00.118	0.083	(1.533E+001)P
0.016	4.600E-003	8.673E-006	1.886E-003	00.116	0.085	(1.583E+001)P
0.017	5.012E-003	8.415E-006	1.679E-003	00.115	0.088	(1.634E+001)P
0.018	5.433E-003	8.162E-006	1.502E-003	00.114	0.090	(1.687E+001)P
0.019	5.862E-003	7.912E-006	1.350E-003	00.112	0.092	(1.741E+001)P
0.020	6.298E-003	7.667E-006	1.217E-003	00.111	0.094	(1.796E+001)P
0.021	6.741E-003	7.427E-006	1.102E-003	00.110	0.096	(1.853E+001)P
0.022	7.190E-003	7.191E-006	1.000E-003	00.109	0.097	(1.911E+001)P
0.023	7.645E-003	6.959E-006	9.103E-004	00.109	0.099	(1.972E+001)P
0.024	8.105E-003	6.732E-006	8.306E-004	00.108	0.101	(2.034E+001)P
0.025	8.570E-003	6.510E-006	7.596E-004	00.107	0.102	(2.098E+001)P
0.026	9.040E-003	6.292E-006	6.961E-004	00.107	0.104	(2.164E+001)P
0.027	9.514E-003	6.080E-006	6.390E-004	00.106	0.105	(2.232E+001)P
0.028	9.992E-003	5.872E-006	5.877E-004	00.105	0.107	(2.302E+001)P
0.029	1.047E-002	5.669E-006	5.413E-004	00.105	0.108	(2.375E+001)P
0.030	1.096E-002	5.472E-006	4.994E-004	00.104	0.110	(2.450E+001)P
0.031	1.144E-002	5.279E-006	4.613E-004	00.104	0.111	(2.528E+001)P
0.032	1.193E-002	5.091E-006	4.266E-004	00.104	0.112	(2.609E+001)P
0.033	1.243E-002	4.909E-006	3.951E-004	00.103	0.113	(2.693E+001)P
0.034	1.292E-002	4.732E-006	3.663E-004	00.103	0.114	(2.779E+001)P
0.035	1.341E-002	4.560E-006	3.399E-004	00.103	0.115	(2.869E+001)P
0.036	1.391E-002	4.394E-006	3.158E-004	00.103	0.116	(2.962E+001)P
0.037	1.441E-002	4.233E-006	2.938E-004	00.102	0.117	(3.058E+001)P
0.038	1.491E-002	4.077E-006	2.735E-004	00.102	0.118	(3.158E+001)P
0.039	1.540E-002	3.927E-006	2.549E-004	00.102	0.119	(3.261E+001)P
0.040	1.590E-002	3.782E-006	2.378E-004	00.102	0.120	(3.368E+001)P
0.041	1.640E-002	3.642E-006	2.221E-004	00.102	0.121	(3.479E+001)P
0.042	1.690E-002	3.508E-006	2.076E-004	00.102	0.122	(3.593E+001)P
0.043	1.740E-002	3.380E-006	1.943E-004	00.102	0.122	(3.710E+001)P
0.044	1.789E-002	3.257E-006	1.820E-004	00.102	0.123	(3.831E+001)P
0.045	1.839E-002	3.140E-006	1.708E-004	00.102	0.124	(3.955E+001)P
0.046	1.888E-002	3.028E-006	1.604E-004	00.102	0.124	(4.082E+001)P
0.047	1.937E-002	2.922E-006	1.508E-004	00.102	0.125	(4.211E+001)P
0.048	1.986E-002	2.822E-006	1.421E-004	00.103	0.125	(4.342E+001)P
0.049	2.035E-002	2.727E-006	1.340E-004	00.103	0.126	(4.475E+001)P

Figure A6. Sample with 0.065 in. radius corresponds to specimen geometry.

Radius of Samples
0.065 in.

CRACK (in.)	Y-BAR (in.^4)	I-BAR (in.^4)	I/y stiffness	b (width)	h (thick)	Stress Intensity (Ksi[in.]^1/2)
0.050	2.083E-002	2.638E-006	1.266E-004	00.103	0.126	(4.609E+001)P
0.051	2.132E-002	2.554E-006	1.198E-004	00.104	0.127	(4.743E+001)P
0.052	2.179E-002	2.476E-006	1.136E-004	00.104	0.127	(4.876E+001)P
0.053	2.227E-002	2.404E-006	1.079E-004	00.104	0.128	(5.009E+001)P
0.054	2.274E-002	2.337E-006	1.028E-004	00.105	0.128	(5.139E+001)P
0.055	2.321E-002	2.275E-006	9.805E-005	00.105	0.128	(5.266E+001)P
0.056	2.367E-002	2.220E-006	9.377E-005	00.106	0.129	(5.390E+001)P
0.057	2.413E-002	2.169E-006	8.991E-005	00.107	0.129	(5.508E+001)P
0.058	2.458E-002	2.124E-006	8.642E-005	00.107	0.129	(5.621E+001)P
0.059	2.503E-002	2.085E-006	8.330E-005	00.108	0.129	(5.727E+001)P
0.060	2.547E-002	2.051E-006	8.052E-005	00.109	0.130	(5.825E+001)P
0.061	2.591E-002	2.022E-006	7.805E-005	00.110	0.130	(5.915E+001)P
0.062	2.634E-002	1.999E-006	7.589E-005	00.111	0.130	(5.996E+001)P
0.063	2.676E-002	1.980E-006	7.400E-005	00.112	0.130	(6.067E+001)P
0.064	2.718E-002	1.967E-006	7.239E-005	00.113	0.130	(6.128E+001)P
0.065	2.759E-002	1.959E-006	7.102E-005	00.114	0.130	(6.179E+001)P
0.066	2.799E-002	1.956E-006	6.989E-005	00.115	0.130	(6.219E+001)P
0.067	2.838E-002	1.958E-006	6.899E-005	00.117	0.130	(6.249E+001)P
0.068	2.877E-002	1.965E-006	6.830E-005	00.118	0.130	(6.269E+001)P
0.069	2.914E-002	1.976E-006	6.781E-005	00.119	0.130	(6.279E+001)P
0.070	2.951E-002	1.992E-006	6.750E-005	00.121	0.130	(6.279E+001)P
0.071	2.987E-002	2.012E-006	6.738E-005	00.123	0.129	(6.271E+001)P
0.072	3.021E-002	2.037E-006	6.743E-005	00.124	0.129	(6.254E+001)P
0.073	3.055E-002	2.066E-006	6.764E-005	00.126	0.129	(6.230E+001)P
0.074	3.088E-002	2.099E-006	6.800E-005	00.128	0.129	(6.200E+001)P
0.075	3.119E-002	2.137E-006	6.850E-005	00.129	0.128	(6.163E+001)P
0.076	3.149E-002	2.177E-006	6.914E-005	00.131	0.128	(6.122E+001)P
0.077	3.178E-002	2.222E-006	6.991E-005	00.133	0.128	(6.077E+001)P
0.078	3.206E-002	2.270E-006	7.081E-005	00.135	0.127	(6.029E+001)P
0.079	3.232E-002	2.321E-006	7.181E-005	00.137	0.127	(5.978E+001)P
0.080	3.257E-002	2.375E-006	7.293E-005	00.139	0.126	(5.926E+001)P
0.081	3.280E-002	2.432E-006	7.415E-005	00.141	0.126	(5.874E+001)P
0.082	3.302E-002	2.492E-006	7.546E-005	00.143	0.125	(5.821E+001)P
0.083	3.322E-002	2.554E-006	7.687E-005	00.145	0.125	(5.769E+001)P
0.084	3.341E-002	2.618E-006	7.836E-005	00.147	0.124	(5.718E+001)P
0.085	3.358E-002	2.684E-006	7.994E-005	00.149	0.124	(5.669E+001)P
0.086	3.373E-002	2.752E-006	8.159E-005	00.152	0.123	(5.623E+001)P
0.087	3.386E-002	2.821E-006	8.331E-005	00.154	0.122	(5.580E+001)P
0.088	3.397E-002	2.891E-006	8.509E-005	00.156	0.122	(5.540E+001)P
0.089	3.406E-002	2.962E-006	8.694E-005	00.158	0.121	(5.504E+001)P
0.090	3.413E-002	3.033E-006	8.885E-005	00.160	0.120	(5.473E+001)P
0.091	3.418E-002	3.104E-006	9.081E-005	00.162	0.119	(5.446E+001)P
0.092	3.421E-002	3.175E-006	9.281E-005	00.164	0.118	(5.424E+001)P
0.093	3.421E-002	3.245E-006	9.487E-005	00.166	0.117	(5.409E+001)P
0.094	3.418E-002	3.314E-006	9.696E-005	00.168	0.116	(5.399E+001)P
0.095	3.413E-002	3.382E-006	9.909E-005	00.171	0.115	(5.395E+001)P
0.096	3.405E-002	3.448E-006	1.013E-004	00.172	0.114	(5.399E+001)P
0.097	3.395E-002	3.512E-006	1.035E-004	00.174	0.113	(5.410E+001)P
0.098	3.381E-002	3.573E-006	1.057E-004	00.176	0.112	(5.428E+001)P

Figure A6. (Cont'd).

Radius of Samples
0.1 in.

CRACK (in.)	Y-BAR (in.^4)	I-BAR (in.^4)	I/y stiffness	b width	h thick	Stress Intensity (Ksi[in.]^1/2)
0.000	0.000E+000	7.854E-005				
0.001	6.096E-005	7.486E-005	1.228E+000	00.400	0.028	(3.144E+000)P
0.002	1.729E-004	7.314E-005	4.231E-001	00.334	0.040	(3.770E+000)P
0.003	3.178E-004	7.170E-005	2.256E-001	00.301	0.049	(4.198E+000)P
0.004	4.891E-004	7.038E-005	1.439E-001	00.279	0.056	(4.535E+000)P
0.005	6.828E-004	6.914E-005	1.013E-001	00.264	0.062	(4.819E+000)P
0.006	8.963E-004	6.795E-005	7.581E-002	00.252	0.068	(5.068E+000)P
0.007	1.128E-003	6.678E-005	5.923E-002	00.242	0.074	(5.292E+000)P
0.008	1.375E-003	6.565E-005	4.775E-002	00.234	0.078	(5.499E+000)P
0.009	1.637E-003	6.453E-005	3.942E-002	00.227	0.083	(5.693E+000)P
0.010	1.913E-003	6.343E-005	3.316E-002	00.221	0.087	(5.876E+000)P
0.011	2.201E-003	6.235E-005	2.832E-002	00.216	0.091	(6.053E+000)P
0.012	2.502E-003	6.127E-005	2.449E-002	00.211	0.095	(6.223E+000)P
0.013	2.813E-003	6.021E-005	2.140E-002	00.207	0.099	(6.390E+000)P
0.014	3.135E-003	5.916E-005	1.887E-002	00.203	0.102	(6.554E+000)P
0.015	3.467E-003	5.812E-005	1.676E-002	00.200	0.105	(6.716E+000)P
0.016	3.809E-003	5.709E-005	1.499E-002	00.197	0.109	(6.877E+000)P
0.017	4.159E-003	5.607E-005	1.348E-002	00.194	0.112	(7.038E+000)P
0.018	4.518E-003	5.505E-005	1.219E-002	00.192	0.114	(7.199E+000)P
0.019	4.885E-003	5.405E-005	1.107E-002	00.189	0.117	(7.360E+000)P
0.020	5.259E-003	5.305E-005	1.009E-002	00.187	0.120	(7.523E+000)P
0.021	5.641E-003	5.207E-005	9.231E-003	00.185	0.123	(7.687E+000)P
0.022	6.029E-003	5.109E-005	8.474E-003	00.183	0.125	(7.853E+000)P
0.023	6.425E-003	5.013E-005	7.802E-003	00.182	0.128	(8.020E+000)P
0.024	6.826E-003	4.917E-005	7.203E-003	00.180	0.130	(8.190E+000)P
0.025	7.234E-003	4.822E-005	6.666E-003	00.179	0.132	(8.363E+000)P
0.026	7.647E-003	4.729E-005	6.184E-003	00.177	0.135	(8.538E+000)P
0.027	8.066E-003	4.636E-005	5.748E-003	00.176	0.137	(8.715E+000)P
0.028	8.490E-003	4.544E-005	5.352E-003	00.175	0.139	(8.896E+000)P
0.029	8.919E-003	4.453E-005	4.993E-003	00.173	0.141	(9.079E+000)P
0.030	9.353E-003	4.364E-005	4.666E-003	00.172	0.143	(9.266E+000)P
0.031	9.791E-003	4.275E-005	4.366E-003	00.171	0.145	(9.456E+000)P
0.032	1.023E-002	4.187E-005	4.092E-003	00.170	0.147	(9.650E+000)P
0.033	1.068E-002	4.101E-005	3.839E-003	00.169	0.148	(9.847E+000)P
0.034	1.113E-002	4.015E-005	3.607E-003	00.168	0.150	(1.005E+001)P
0.035	1.159E-002	3.931E-005	3.393E-003	00.167	0.152	(1.025E+001)P
0.036	1.204E-002	3.847E-005	3.195E-003	00.167	0.154	(1.046E+001)P
0.037	1.250E-002	3.765E-005	3.011E-003	00.166	0.155	(1.067E+001)P
0.038	1.297E-002	3.684E-005	2.840E-003	00.165	0.157	(1.089E+001)P
0.039	1.344E-002	3.604E-005	2.682E-003	00.165	0.158	(1.111E+001)P
0.040	1.391E-002	3.525E-005	2.535E-003	00.164	0.160	(1.134E+001)P
0.041	1.438E-002	3.447E-005	2.397E-003	00.163	0.161	(1.157E+001)P
0.042	1.486E-002	3.371E-005	2.269E-003	00.163	0.163	(1.180E+001)P
0.043	1.533E-002	3.295E-005	2.149E-003	00.162	0.164	(1.205E+001)P
0.044	1.582E-002	3.221E-005	2.037E-003	00.162	0.166	(1.229E+001)P
0.045	1.630E-002	3.148E-005	1.932E-003	00.161	0.167	(1.254E+001)P
0.046	1.678E-002	3.076E-005	1.833E-003	00.161	0.168	(1.280E+001)P
0.047	1.727E-002	3.006E-005	1.740E-003	00.160	0.170	(1.306E+001)P
0.048	1.776E-002	2.936E-005	1.653E-003	00.160	0.171	(1.333E+001)P
0.049	1.825E-002	2.868E-005	1.572E-003	00.160	0.172	(1.361E+001)P

Figure A7. Sample with 0.1 in. radius corresponds to actual wire geometry.

Radius of Samples
0.1 in

CRACK <in.>	Y-BAR <in.^4>	I-BAR <in.^4>	I/A stiffness	b <width>	h <thick>	Stress Intensity <Ksi[in.]^1/2>
0.050	1.874E-002	2.801E-005	1.495E-003	00.159	0.173	(1.389E+001)P
0.051	1.923E-002	2.735E-005	1.422E-003	00.159	0.174	(1.418E+001)P
0.052	1.972E-002	2.671E-005	1.354E-003	00.159	0.175	(1.447E+001)P
0.053	2.022E-002	2.607E-005	1.290E-003	00.158	0.177	(1.477E+001)P
0.054	2.071E-002	2.545E-005	1.229E-003	00.158	0.178	(1.508E+001)P
0.055	2.121E-002	2.484E-005	1.171E-003	00.158	0.179	(1.540E+001)P
0.056	2.171E-002	2.425E-005	1.117E-003	00.158	0.180	(1.572E+001)P
0.057	2.221E-002	2.367E-005	1.066E-003	00.158	0.181	(1.605E+001)P
0.058	2.270E-002	2.310E-005	1.017E-003	00.157	0.182	(1.639E+001)P
0.059	2.320E-002	2.254E-005	9.715E-004	00.157	0.182	(1.674E+001)P
0.060	2.370E-002	2.200E-005	9.281E-004	00.157	0.183	(1.709E+001)P
0.061	2.420E-002	2.147E-005	8.871E-004	00.157	0.184	(1.745E+001)P
0.062	2.470E-002	2.095E-005	8.482E-004	00.157	0.185	(1.782E+001)P
0.063	2.520E-002	2.044E-005	8.114E-004	00.157	0.186	(1.820E+001)P
0.064	2.569E-002	1.995E-005	7.765E-004	00.157	0.187	(1.859E+001)P
0.065	2.619E-002	1.947E-005	7.434E-004	00.157	0.187	(1.898E+001)P
0.066	2.669E-002	1.901E-005	7.121E-004	00.157	0.188	(1.938E+001)P
0.067	2.718E-002	1.855E-005	6.825E-004	00.157	0.189	(1.979E+001)P
0.068	2.768E-002	1.811E-005	6.544E-004	00.157	0.189	(2.021E+001)P
0.069	2.818E-002	1.769E-005	6.277E-004	00.157	0.190	(2.063E+001)P
0.070	2.867E-002	1.727E-005	6.025E-004	00.157	0.191	(2.106E+001)P
0.071	2.916E-002	1.687E-005	5.786E-004	00.157	0.191	(2.149E+001)P
0.072	2.965E-002	1.649E-005	5.560E-004	00.158	0.192	(2.193E+001)P
0.073	3.014E-002	1.611E-005	5.346E-004	00.158	0.193	(2.238E+001)P
0.074	3.063E-002	1.575E-005	5.143E-004	00.158	0.193	(2.282E+001)P
0.075	3.112E-002	1.541E-005	4.951E-004	00.158	0.194	(2.328E+001)P
0.076	3.161E-002	1.507E-005	4.769E-004	00.159	0.194	(2.373E+001)P
0.077	3.209E-002	1.475E-005	4.597E-004	00.159	0.195	(2.419E+001)P
0.078	3.257E-002	1.445E-005	4.435E-004	00.159	0.195	(2.464E+001)P
0.079	3.305E-002	1.415E-005	4.282E-004	00.160	0.196	(2.510E+001)P
0.080	3.353E-002	1.387E-005	4.137E-004	00.160	0.196	(2.555E+001)P
0.081	3.401E-002	1.360E-005	4.001E-004	00.160	0.196	(2.601E+001)P
0.082	3.448E-002	1.335E-005	3.872E-004	00.161	0.197	(2.645E+001)P
0.083	3.495E-002	1.311E-005	3.751E-004	00.161	0.197	(2.690E+001)P
0.084	3.542E-002	1.288E-005	3.637E-004	00.162	0.197	(2.733E+001)P
0.085	3.588E-002	1.267E-005	3.530E-004	00.162	0.198	(2.776E+001)P
0.086	3.635E-002	1.246E-005	3.429E-004	00.163	0.198	(2.818E+001)P
0.087	3.681E-002	1.228E-005	3.335E-004	00.164	0.198	(2.859E+001)P
0.088	3.726E-002	1.210E-005	3.247E-004	00.164	0.199	(2.899E+001)P
0.089	3.771E-002	1.194E-005	3.165E-004	00.165	0.199	(2.937E+001)P
0.090	3.816E-002	1.179E-005	3.089E-004	00.166	0.199	(2.974E+001)P
0.091	3.861E-002	1.165E-005	3.017E-004	00.167	0.199	(3.009E+001)P
0.092	3.905E-002	1.153E-005	2.951E-004	00.167	0.199	(3.043E+001)P
0.093	3.949E-002	1.141E-005	2.890E-004	00.168	0.200	(3.074E+001)P
0.094	3.993E-002	1.131E-005	2.834E-004	00.169	0.200	(3.104E+001)P
0.095	4.036E-002	1.123E-005	2.782E-004	00.170	0.200	(3.132E+001)P
0.096	4.078E-002	1.115E-005	2.735E-004	00.171	0.200	(3.158E+001)P
0.097	4.120E-002	1.109E-005	2.692E-004	00.172	0.200	(3.181E+001)P
0.098	4.162E-002	1.104E-005	2.652E-004	00.173	0.200	(3.202E+001)P

Figure A7. (Cont'd).

Radius of Samples
0.1 in

CRACK <in.>	Y-BAR <in.^4>	I-BAR <in.^4>	I/> stiffness	b <width>	h <thick>	Stress Intensity <Ksi[in.]^1/2>
0.050	1.874E-002	2.801E-005	1.495E-003	00.159	0.173	(1.389E+001)P
0.051	1.923E-032	2.735E-005	1.422E-003	00.159	0.174	(1.418E+001)P
0.052	1.972E-002	2.671E-005	1.354E-003	00.159	0.175	(1.447E+001)P
0.053	2.022E-002	2.607E-005	1.290E-003	00.158	0.177	(1.477E+001)P
0.054	2.071E-002	2.545E-005	1.229E-003	00.158	0.178	(1.508E+001)P
0.055	2.121E-002	2.484E-005	1.171E-003	00.158	0.179	(1.540E+001)P
0.056	2.171E-002	2.425E-005	1.117E-003	00.158	0.180	(1.572E+001)P
0.057	2.221E-002	2.367E-005	1.066E-003	00.158	0.181	(1.605E+001)P
0.058	2.270E-002	2.310E-005	1.017E-003	00.157	0.182	(1.639E+001)P
0.059	2.320E-002	2.254E-005	9.715E-004	00.157	0.182	(1.674E+001)P
0.060	2.370E-002	2.200E-005	9.281E-004	00.157	0.183	(1.709E+001)P
0.061	2.420E-002	2.147E-005	8.871E-004	00.157	0.184	(1.745E+001)P
0.062	2.470E-002	2.095E-005	8.482E-004	00.157	0.185	(1.782E+001)P
0.063	2.520E-002	2.044E-005	8.114E-004	00.157	0.186	(1.820E+001)P
0.064	2.569E-002	1.995E-005	7.765E-004	00.157	0.187	(1.859E+001)P
0.065	2.619E-002	1.947E-005	7.434E-004	00.157	0.187	(1.898E+001)P
0.066	2.669E-002	1.901E-005	7.121E-004	00.157	0.188	(1.938E+001)P
0.067	2.718E-002	1.855E-005	6.825E-004	00.157	0.189	(1.979E+001)P
0.068	2.768E-002	1.811E-005	6.544E-004	00.157	0.189	(2.021E+001)P
0.069	2.818E-002	1.769E-005	6.277E-004	00.157	0.190	(2.063E+001)P
0.070	2.867E-002	1.727E-005	6.025E-004	00.157	0.191	(2.106E+001)P
0.071	2.916E-002	1.687E-005	5.786E-004	00.157	0.191	(2.149E+001)P
0.072	2.965E-002	1.649E-005	5.560E-004	00.158	0.192	(2.193E+001)P
0.073	3.014E-002	1.611E-005	5.346E-004	00.158	0.193	(2.238E+001)P
0.074	3.063E-002	1.575E-005	5.143E-004	00.158	0.193	(2.282E+001)P
0.075	3.112E-002	1.541E-005	4.951E-004	00.158	0.194	(2.328E+001)P
0.076	3.161E-002	1.507E-005	4.769E-004	00.159	0.194	(2.373E+001)P
0.077	3.209E-002	1.475E-005	4.597E-004	00.159	0.195	(2.419E+001)P
0.078	3.257E-002	1.445E-005	4.435E-004	00.159	0.195	(2.464E+001)P
0.079	3.305E-002	1.415E-005	4.282E-004	00.160	0.196	(2.510E+001)P
0.080	3.353E-002	1.387E-005	4.137E-004	00.160	0.196	(2.555E+001)P
0.081	3.401E-002	1.360E-005	4.001E-004	00.160	0.196	(2.601E+001)P
0.082	3.448E-002	1.335E-005	3.872E-004	00.161	0.197	(2.645E+001)P
0.083	3.495E-002	1.311E-005	3.751E-004	00.161	0.197	(2.690E+001)P
0.084	3.542E-002	1.288E-005	3.637E-004	00.162	0.197	(2.733E+001)P
0.085	3.588E-002	1.267E-005	3.530E-004	00.162	0.198	(2.776E+001)P
0.086	3.635E-002	1.246E-005	3.429E-004	00.163	0.198	(2.818E+001)P
0.087	3.681E-002	1.228E-005	3.335E-004	00.164	0.198	(2.859E+001)P
0.088	3.726E-002	1.210E-005	3.247E-004	00.164	0.199	(2.899E+001)P
0.089	3.771E-002	1.194E-005	3.165E-004	00.165	0.199	(2.937E+001)P
0.090	3.816E-002	1.179E-005	3.089E-004	00.166	0.199	(2.974E+001)P
0.091	3.861E-002	1.165E-005	3.017E-004	00.167	0.199	(3.009E+001)P
0.092	3.905E-002	1.153E-005	2.951E-004	00.167	0.199	(3.043E+001)P
0.093	3.949E-002	1.141E-005	2.890E-004	00.168	0.200	(3.074E+001)P
0.094	3.993E-002	1.131E-005	2.834E-004	00.169	0.200	(3.104E+001)P
0.095	4.036E-002	1.123E-005	2.782E-004	00.170	0.200	(3.132E+001)P
0.096	4.078E-002	1.115E-005	2.735E-004	00.171	0.200	(3.158E+001)P
0.097	4.120E-002	1.109E-005	2.692E-004	00.172	0.200	(3.181E+001)P
0.098	4.162E-002	1.104E-005	2.652E-004	00.173	0.200	(3.202E+001)P

Figure A7. (Cont'd).

CERL DISTRIBUTION

Chief of Engineers
ATTN: Tech Monitor
ATTN: DAEN-ASI-L (2)
ATTN: DAEN-CCP
ATTN: DAEN-CW
ATTN: DAEN-CWE
ATTN: DAEN-CWM-R
ATTN: DAEN-CWO
ATTN: DAEN-CWP
ATTN: DAEN-EC
ATTN: DAEN-ECC
ATTN: DAEN-ECE
ATTN: DAEN-ZCF
ATTN: DAEN-ECI
ATTN: DAEN-RD
ATTN: DAEN-RDC
ATTN: DAEN-RDM
ATTN: DAEN-RM
ATTN: DAEN-ZCZ
ATTN: DAEN-ZCE
ATTN: DAEN-ZCI
ATTN: DAEN-ZCM

FESA, ATTN: Library 22060
ATTN: DET III 79906

US Army Engineer Districts
ATTN: Library (41)

US Army Engineer Divisions
ATTN: Library (14)

US Army Europe
AEAEN-ODCS/Engr 09403
ISAE 09081
V Corps
ATTN: DEH (11)
VII Corps
ATTN: DEH (15)
21st Support Command
ATTN: DEH (12)
USA Berlin
ATTN: DEH (15)
USASETAF
ATTN: DEH (6)
Allied Command Europe (ACE)
ATTN: DEH (3)

8th USA, Korea (14)

ROK/US Combined Forces Command 96301
ATTN: EUSA-HHC-CFC/Engr

USA Japan (USARJ)
ATTN: AJEN-FE 96343
ATTN: DEH-Honshu 96343
ATTN: DEH-Okinawa 96331

Area Engineer, AEDC-Area Office
Arnold Air Force Station, TN 37389

416th Engineer Command 60623
ATTN: Facilities Engineer

US Military Academy 10966
ATTN: Facilities Engineer
ATTN: Dept of Geography & Computer Science
ATTN: DSCPER/MAEN-A

AMMRC, ATTN: DRXMR-WE 02172

USA ARRCOM 61299
ATTN: DRCIS-RI-I
ATTN: DRSAR-IS

DARCOM - Dir., Inst., & Svcs.
ATTN: DEH (23)

DLA, ATTN: DLA-WI 22314

FORSCOM
FORSCOM Engineer, ATTN: AFEN-DEH
ATTN: DEH (23)

HSC
ATTN: HSLO-F 78234
ATTN: Facilities Engineer
Fitzsimons AMC 80240
Walter Reed AMC 20012

INSCOM - Ch, Instl. Div.
ATTN: Facilities Engineer (3)

MDW
ATTN: DEH (3)

MTMC
ATTN: MTMC-SA 20315
ATTN: Facilities Engineer (3)

NARADCOM, ATTN: DRDNA-F 071160

TARCOM, Fac. Div. 48090

TRADOC
HQ, TRADOC, ATTN: ATEN-DEH
ATTN: DEH (19)

TSARCOM, ATTN: STSAS-F 63120

USACC
ATTN: Facilities Engineer (2)

WESTCOM
ATTN: DEH
Fort Shafter 96858
ATTN: APEN-IM

SHAPE 09055
ATTN: Survivability Section, CCB-OPS
Infrastructure Branch, LANDA

HQ USEUCOM 09128
ATTN: ECJ 4/7-LOE

U.S. Army, Fort Belvoir 22060
ATTN: Canadian Liaison Officer
ATTN: Water Resources Support Center
ATTN: Engr Studies Center
ATTN: Engr Topographic Lab
ATTN: ATZA-DTE-SU
ATTN: ATZA-DTE-EM
ATTN: R & D Command

CRREL, ATTN: Library 03755

WES, ATTN: Library 39180

HQ, XVIII Airborne Corps and
Ft. Bragg 28307
ATTN: AFZA-FE-EE

Chanute AFB, IL 61868
3345 CES/DE, Stop 27

Norton AFB CA 92409
ATTN: AFRCE-MX/DEE

Tyndall AFB, FL 32403
AFESC/Engineering & Service Lab

NAVFAC
ATTN: ROT&E Liaison Office (6)
ATTN: Sr. Tech. FAC-03T 22332
ATTN: Asst. CDR R&D, FAC-03 22332

NCEL 93041
ATTN: Library (Code L08A)

Defense Technical Info. Center 22314
ATTN: DDA (12)

Engineering Societies Library
New York, NY 10017

National Guard Bureau 20310
Installation Division

US Government Printing Office 22304
Receiving Section/Depository Copies (2)

US Army Env. Hygiene Agency
ATTN: HSHB-E 21010

National Bureau of Standards 20760

1 4/84

Metallurgy Team Distribution

Chief of Engineers
ATTN: DAEN-ZCF-U
ATTN: DAEN-ECZ-A
ATTN: DAEN-ECB

US Army Engineer District
Philadelphia 19106
ATTN: Chief, NAPEN-D
Baltimore 21203
ATTN: Chief, Engr Div
Norfolk 23510
ATTN: Chief, NAOEN-D
Wilmington 28401
ATTN: Chief, SAWEN-D
Charleston 29402
ATTN: Chief, Engr Div
Savannah 31402
ATTN: Chief, SASAS-L
Jacksonville 32232
ATTN: Const Div
Mobile 36628
ATTN: Chief, SAMEN-C
ATTN: Chief, SAMEN-D
Memphis 38103
ATTN: Chief, LMMED-DM
Vicksburg 39180
ATTN: Chief, Engr Div
Louisville 40201
ATTN: Chief, Engr Div
St. Paul 55101
ATTN: Chief, ED-D
Omaha 68102
ATTN: Chief, Engr Div
New Orleans 70160
ATTN: Chief, LMNED-DG
Little Rock 72203
ATTN: Chief, Engr Div
San Francisco 94105
ATTN: Chief, Engr Div
Sacramento 95814
ATTN: Chief, SPKED-D
Portland 97208
ATTN: Chief, DB-6
Seattle 98124
ATTN: Chief, NPSCO
Walla Walla 99362
ATTN: Chief, Engr Div
Alaska 99501
ATTN: Chief, NPASA-R

US Army Engineer Division
New England
ATTN: Chief, NEDED-T
North Atlantic 10007
ATTN: Chief, NADEN-T
South Atlantic 30303
ATTN: Chief, SADEN-TS
Huntsville 35807
ATTN: Chief, HNDED-CS
ATTN: Chief, HNDED-SR
Ohio River 45201
ATTN: Chief, Engr Div
Southwestern 75202
ATTN: SWDED-TM
Pacific Ocean 96858
ATTN: Chief, Engr Div
North Pacific 97208
ATTN: Chief, Engr Div

USA-WES 39180
ATTN: C/Structures

West Point, NY 10996
ATTN: Dept of Mechanics
ATTN: Library

Fort Leavenworth, KS 66027
ATTN: ATZLCA-SA

Fort Clayton Canal Zone 34004
ATTN: DFAE

Fort McPherson, GA 30330
ATTN: AFEN-CD

Fort Monroe, VA 23651
ATTN: ATEN-AD (3)

6th US Army 94129
ATTN: AFKC-EN

7th US Army 09407
ATTN: AETTM-HRD-EHD

US Army Science & Technology 96301
Center - Far East Office

Tyndall AFB, FL 32403
AFESC/PRT

Tinker AFB, OK 73145
2854 ABG/DEEE

Patrick AFB, FL 32925
ATTN: XRQ

Naval Air Systems Command 20360
ATTN: Library

Naval Facilities Engr Command 22332
ATTN: Code 04

Transportation Research Board 20418

Dept of Transportation Library 20590

National Defense Headquarters
Ottawa, CANADA K1A 0K2

Airports and Construction Services Dir
Ottawa, CANADA K1A 0N8

Segan, Ellen G.
Assessment of the stress corrosion cracking of post-tensioned tendons at the John Day Lock / by E. G. Segan, D. Socie, D. Morrow. - Champaign, IL : Construction Engineering Research Laboratory ; available from NTIS, 1984.
26 p. (Technical report / Construction Engineering Research Laboratory ; M-349)

1. John Day Lock. 2. Locks (hydraulic engineering) 3. Stress corrosion. I. Socie, D. II. Morrow D. III. Title. IV. Series : Technical report (Construction Engineering Research Laboratory) ; M-349.

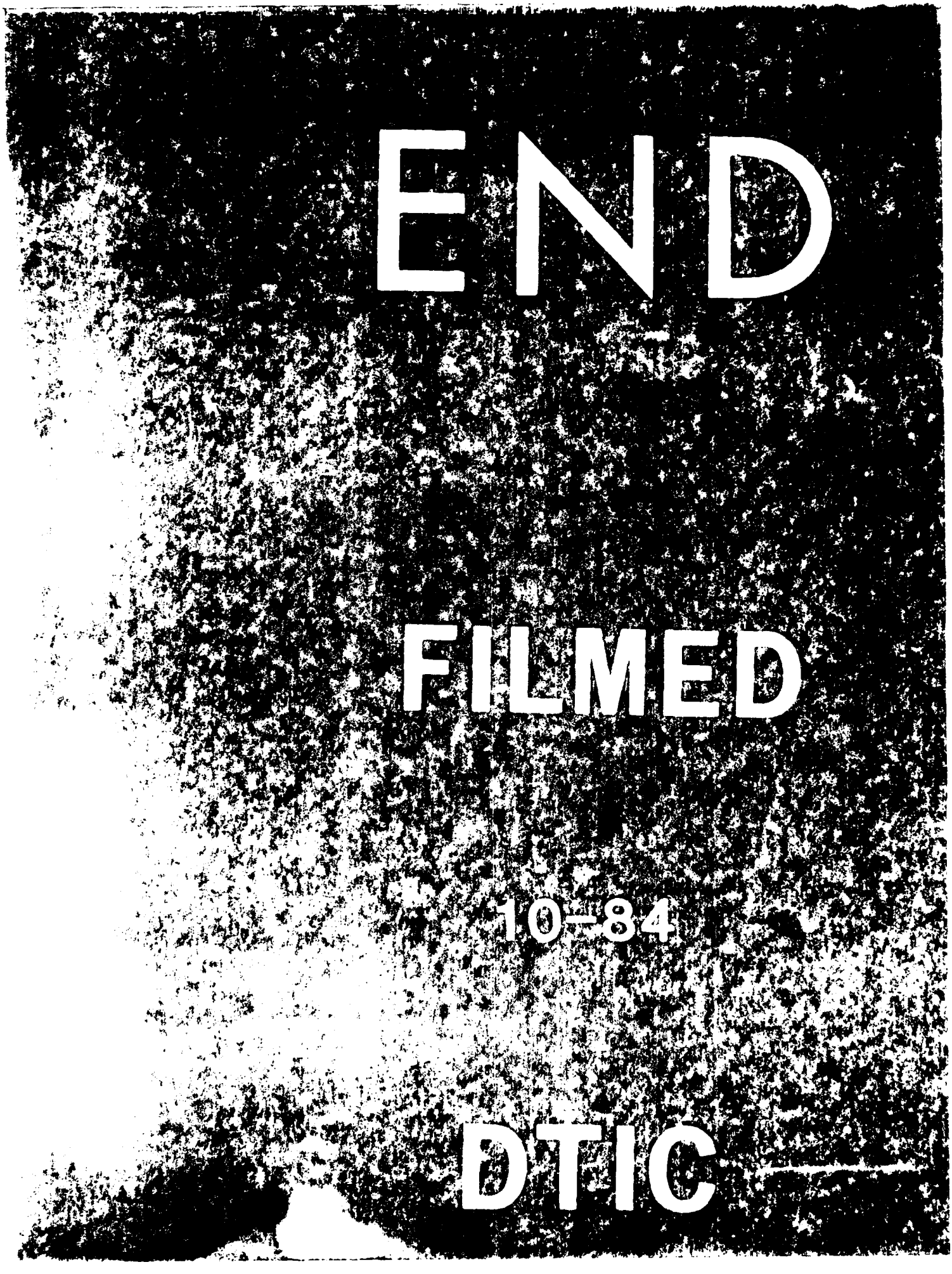
END
FILMED
10-84
DTIC